arXiv:1410.2449v1 [astro-ph.SR] 9 Oct 2014

# Photometric analysis of overcontact binaries AK Her, HI Dra, V1128 Tau and V2612 Oph

Ş. Çalışkan

Department of Astronomy & Space Sciences, Faculty of Science, Ankara University, TR-06100 Tandogan, Ankara, Turkey

seyma.caliskan@science.ankara.edu.tr

O. Latković

Astronomical Observatory, Volgina 7, 11060 Belgrade, Serbia

olivia@aob.rs

G. Djurašević[1]

Astronomical Observatory, Volgina 7, 11060 Belgrade, Serbia

gdjurasevic@aob.rs

İ. Özavcı

Department of Astronomy & Space Sciences, Faculty of Science, Ankara University, TR-06100 Tandogan, Ankara, Turkey

ozavci@science.ankara.edu.tr

Ö. Baştürk

Department of Astronomy & Space Sciences, Faculty of Science, Ankara University, TR-06100 Tandogan, Ankara, Turkey

obasturk@ankara.edu.tr

[1]Isaac Newton Institute of Chile, Yugoslavia Branch

A. Cséki

Astronomical Observatory, Volgina 7, 11060 Belgrade, Serbia

attila@aob.rs

H. V. Şenavcı

Department of Astronomy & Space Sciences, Faculty of Science, Ankara University, TR-06100 Tandogan, Ankara, Turkey

hvsenavci@ankara.edu.tr

T. Kılıçoğlu

Department of Astronomy & Space Sciences, Faculty of Science, Ankara University, TR-06100 Tandogan, Ankara, Turkey

tkilicoglu@ankara.edu.tr

M. Yılmaz

Department of Astronomy & Space Sciences, Faculty of Science, Ankara University, TR-06100 Tandogan, Ankara, Turkey

mesutyilmaz@ankara.edu.tr

and

S. O. Selam

Department of Astronomy & Space Sciences, Faculty of Science, Ankara University, TR-06100 Tandogan, Ankara, Turkey

selam@science.ankara.edu.tr

Received _____; accepted _____

## ABSTRACT

We analyze new, high quality multicolor light curves of four overcontact binaries: AK Her, HI Dra, V1128 Tau and V2612 Oph, and determine their orbital and physical parameters using the modeling program of G. Djurasevic and recently published results of radial velocity studies. The achieved precision in absolute masses is between 10 and 20%, and in absolute radii between 5 and 10%. All four systems are W UMa type binaries with bright or dark spots indicative of mass and energy transfer or surface activity. We estimate the distances and the ages of the systems using the luminosities computed through our analysis, and perform an O-C study for V1128 Tau, which reveals a complex period variation that can be interpreted in terms of mass loss/exchange and either the presence of the third body, or the magnetic activity on one of the components. We conclude that further observations of these systems are needed to deepen our understanding of their nature and variability.


*Subject headings:* binaries: eclipsing – binaries: close – stars: fundamental parameters – stars: individual: AK Her, HI Dra, V1128 Tau, V2612 Oph

## 1. Introduction

Overcontact binaries are close binary star systems in which one of the components has become engulfed in the expanding envelope of its evolving companion. The two stars are virtually indistinguishable and often appear to be of same effective temperatures, since they share a common envelope and are typically located at a separation of the same order of magnitude as the stellar radii. However, the components of overcontact systems are stars of different masses and at different evolutionary stages, with the added caveat that their evolution has been affected by the proximity of their companion. In fact, it is not uncommon to find overcontact systems in which the originally less massive component is now observed to be the more massive one thanks to accumulating the material lost during its companion‘s evolution-driven expansion. This phenomenon, often referred to as the mass ratio reversal, can in principle happen more than once in the same system. Yet it's only one of the many astrophysically interesting processes that can be inferred from the study of overcontact systems, like the exchange of energy and angular momentum, mass loss, interaction of stellar winds, magnetic activity and so forth. On the other hand, the small separation makes it more probable that an overcontact system will also be found to be eclipsing, which allows precise determination of orbital and stellar parameters from photometric light curves through the well-established methods for modeling of binary stars. Considering all this, it is clear why the case studies of bright, eclipsing overcontact binaries remain attractive even in the era of space telescopes and massive surveys.

In this paper we present the analysis of new, high quality CCD light curves, based on the results of up to date radial velocity studies of four overcontact eclipsing binaries: AK Her, HI Dra, V1128 Tau and V2612 Oph. Our findings suggest that AK Her and V2612 Oph belong to the A subtype of W UMa binaries, while HI Dra and V1128 Tau are of W-subtype. In all four solutions, we use dark or bright spots on one or both components

to explain the asymmetries of the light curves. These inhomogeneities in surface brightness can be explained as either arising from photospheric activity, or resulting from mass and energy transfer.

In addition to constraining the absolute masses and radii of the components of these four systems, we update their ephemerides using newly measured times of minimum light combined with all the previous measurements found in literature and calculate the distances based on the computed luminosities resulting from our models. We then estimate the age of each system by employing a novel method developed specifically for W UMa type binaries (Yıldız 2014). The age calculation is based on the estimated initial mass of the less massive secondary star, which can in turn be infered from the departure of its size and luminosity from values expected in a main sequence star of its mass (see the cited work and the references within for a detailed explanation).

Finally, we perform a period study for V1128 Tau based on the O-C diagram constructed with all the available times of minimum light. We find the period variation can be fitted well with a superposition of a quadratic and a cyclic function, indicative of both mass transfer and either a third body in the system or magnetic activity on one of the components.

In what follows, we describe the technical details of the observations (Section 2) and the light curve analysis (Section 3), and then each system is discussed in turn. A summary of our results can be inspected at a glance from Figures 1, 2, 3 and 4, as well as from the concluding remarks given in Section 8.

## 2. Observations

We obtained CCD photometric observations of our objects with the Apogee ALTA U47 CCD camera attached to the 40 cm Schmidt-Cassegrain telescope at the Ankara University Kreiken Observatory (AUKR), using the wideband BVRI filters of Johnson-Cousins system.

The bias subtraction, dark and flat corrections were applied to the object images by the IRAF[1] task CCDPROC. We then performed aparture photometry with the relevant tasks in the IRAF/APPHOT package on each individual calibrated frames.

The magnitudes and their errors in each band were computed in the sense of variable minus comparison (V-C). We determined the nightly extinction coefficients for the magnitudes from the comparison stars.

The light curves were phased using the light elements calculated from newly observed and archival times of minima. The light elements, comparison stars, and the uncertainties of the observations are listed in Table 1, and the times of minimum light newly derived from our observations are given in Table 2. A preview of the data is given in Table 3, and the full light curves are available as a machine-readable table in the online version of the journal.

## 3. Light curve analysis

Light curve analysis was done with the version of the program by Djurašević (1992a) generalized for the case of overcontact configurations (Djurašević et al. 1998). The underlying model is based on the Roche geometry, and the orbital and stellar parameters

[1]IRAF is distributed by the National Optical Astronomy Observatories, which are operated by the Association of Universities for Research in Astronomy, Inc., under cooperative agreement with the National Science Foundation.

are estimated by solving the inverse problem with a modified Marquardt (1963) algorithm. More details about the model and parameter determination can be found in Djurašević (1992b).

Our results are summarized in Tables 4, 5, 6, and 7. In the interest of limiting the parameter space and better constraining the solution, certain parameters were fixed to values obtained through independent analysis of radial velocity curves or to theoretical values based on plausible assumptions about the components. Below is a list with all the model parameters (with adopted values where applicable) and explanations of used notation:

- Point count — the total number of the observations spanning all the passbands.
- $\sigma$ — the standard deviation of the residuals.
- $\mathrm{q} = \mathrm{m_2/m_1}$ — the mass ratio of the components. The index 1 always marks the more massive component, so that the mass ratio is always less than one. This parameter was kept constant, with the value adopted from recent radial velocity studies: $q = 0.277 \pm 0.024$ for AK Her, from Pribulla et al. (2006); $q = 0.250 \pm 0.005$ for HI Dra, from Pribulla et al. (2009); $q = 0.534 \pm 0.006$ for V1128 Tau, from Rucinski et al. (2008); and $q = 0.286 \pm 0.003$ for V2162 Oph, from Pribulla et al. (2007).
- i — the orbital inclination (in degrees).
- $\mathrm{a_{orb}}$ — the orbital semi-major axis in units of solar radius (where the value of $\mathrm{a \cdot \sin(i)}$ adopted from the radial velocity studies mentioned above).
- d — the distance to the object in parsecs.
- $\ell_3/(\ell_1 + \ell_2 + \ell_3)$ — the contribution of uneclipsed (third) light to the total light of the system at the phase of the light-curve maximum (omitted when zero).
- $\mathrm{f_{over}}$ — the degree of overcontact (in percents), defined as $f_{over} = 100\frac{\Omega - \Omega_{in}}{\Omega_{out} - \Omega_{in}}$, where $\Omega$, $\Omega_{\mathrm{in}}$ and $\Omega_{\mathrm{out}}$ are the dimensionless surface potentials of the common photosphere and the inner and outer critical surfaces, respectively (omitted in detached systems).
- $\Omega_{\mathrm{in}}$ and $\Omega_{\mathrm{out}}$ — the dimensionless values of Roche potential at the inner and outer critical surfaces that contain the equilibrium points $\mathrm{L_1}$ and $\mathrm{L_2}$, respectively (omitted in detached systems).

- A, $\beta$ — the albedo and the gravity-darkening exponent of the component. These parameters were fixed to their theoretical values (see Lucy 1967; von Zeipel 1924), according to the the temperature inferred from the spectral classification for the primary, and a preliminary estimate of the temperature of the secondary.
- $f = \omega/\omega_K$ — the ratio of the rotation rate of the component to the Keplerian orbital rate. This parameter was fixed to the value of $f = 1$ for all systems, along the assumption that the rotation of the components is synchronous with the orbital revolution since the tidal effects are expected to lead to the synchronization of the rotational and orbital periods in such close systems.
- $\mathrm{T_{eff}}$ — the effective temperature of the component (in Kelvins), corresponding to the average of local temperatures weighted by the areas of elementary surfaces. It is usually estimated from spectral classification for one component (according to the revised theoretical $\mathrm{T_{eff}}$–spectral-type calibration by Martins, Schaerer & Hillier 2005), and adjusted as a parameter of the model for the other.
- F — the filling factor of the component, defined as the ratio between the stellar polar radius and the polar radius of the critical Roche surface.
- $\Omega$ — the dimensionless surface potential of the component.
- $\mathrm{L}/(\mathrm{L_1} + \mathrm{L_2})$ — the contribution of the component to the total luminosity of the system.
- R — the polar radius of the component in units of separation.
- $\mathcal{M}$, $\mathcal{R}$ — the mass and the mean radius of the component in solar units.
- $\log \mathrm{g}$ — the logarithm (to base ten) of the effective gravity of the component in CGS units.
- $\mathrm{M_{bol}}$ — the absolute bolometric magnitude of the component.
- $\mathrm{T_{spot}}/\mathrm{T}$ — the ratio between the temperature of the spot and the local temperature of the star.
- $\theta$, $\lambda$, $\varphi$ — the angular radius, longitude, and latitude of the spot (in arc degrees). The longitude ($\lambda$) is measured in the orbital plane, from the $+x$ axis (the line connecting the centers of the components), clockwise as viewed from the "north" ($+z$) pole, in the range from 0° to 360°. The latitude ($\varphi$) is measured from 0° at the the orbital plane to 90° towards the "north" ($+z$) pole and $-90°$ towards the "south" ($-z$) pole.

Limb darkening is calculated according to the nonlinear approximation of Claret & Bloemen (2011), with the coefficients for the appropriate passbands interpolated from their tables based on the values of $\mathrm{T_{eff}}$ and log g in each iteration.

The distances are computed based on the apparent magnitudes taken from the SIMBAD database[2], published by van Leeuwen (2007) for all stars except V2612 Oph, for which the SIMBAD database has no published source; and from the computed absolute magnitudes, with corrections for the interstellar extinction. The interstellar extinction values ($A_v$) in the V passband are calculated using the reddening values estimated from the infrared dust emission maps of Schlegel et al. (1998) and by assuming an extinction to reddening ratio of $A_v/E(B-V)$ of 3.1. Note that Schlegel et al. (1998) refer to the total absorption. The bolometric corrections are taken from the tables published by Flower (1996), according to the computed effective temperatures of the components for each system.

We use the methods prescribed by Yıldız (2014) to estimate the inital masses and ages of the systems, and classify them as either the A or W subtypes of W UMa binaries according to the criteria introduced by Binnendijk (1970).

The uncertainties reported in Tables 4, 5, 6, 7 and throughout the text are derived from the formal fitting errors.

In the following sections we present the results of our work for each system in turn.

## 4. AK Her

AK Her (HD 155937, BD+16 3130, HIP 84293, SAO 102688, GSC 1536-1738) is an overcontact eclipsing binary with the orbital period of $P = 0.421522$ days. It's the brighter component of the visual binary ADS 10408. The visual companion is a physical member of the system, separated by 4.7 arcseconds and 3.5 mag fainter than AK Her at

[2]http://simbad.u-strasbg.fr/simbad/

maximum light. It has been associated with a weak X-ray source (Cruddace & Dupree 1984; McGale et al. 1996), which is an indication of coronal activity. Numerous authors published photometric light curves and times of minimum light. The variability of the orbital period was first noted by Woodward (1941). Schmidt & Herczeg (1959) did a through analysis of the variations in the light curves during the years prior to their study. They pointed out the changing levels of light curve minima and maxima, as well as the variability in spectral types and color indices, and ruled out the distant visual companion as the cause of period variation. A detailed study of the period changes was performed by Li et al. (2001), who found a long-term decrease and three rapid components of the variation. They interpret the slow variability in terms of mass exhange, and the rapid variations as pulsations of the common envelope. More recently, Samadi et al. (2010) analyzed multicolor light curves of AK Her together with the radial velocity data from Sanford (1934) and calculated the absolute parameters. Based on the O-C analysis, they measure the amplitudes and frequencies of the three componenst of orbital period variation, and interpret them in terms of the presence of the third body and magnetic activity.

A spectroscopic study of AK Her was done by Pribulla et al. (2006). The authors classified the brighter star as F4 V and measured the spectroscopic mass ratio of $q = 0.277$, which is the value used in this work. Although they did not detect the signature of additional components in the spectra, they too argue, based on the observed light-time effect, that there must be an unseen companion to the system much closer than the visual pair. However, it has not yet been directly observed.

The present analysis of $BVR_CI_C$ light curves results in a model of AK Her in which the more massive, larger and hotter (primary) star is the one eclipsed in the deeper minimum (Figure 1). This makes AK Her a member of the A subtype of W UMa binaries. From the summary of results given in Table 4 it can be seen that the mass and the radius of

the primary are near the expected values for a main sequence star of spectral class F4 V, adopted from Pribulla et al. (2006), while the secondary is too large and overluminous for a main sequence star of its mass. This is a common observational characteristic of overcontact systems. We find the degree of overcontact is 33.2%, and place two dark spots that likely arise from surface activity on the primary star to account for the light curve assymetries. There is a significant contribution of uneclipsed light, probably from the unresolved third body.

These results are in reasonable agreement with the findings of previous studies. In comparison with the most recent one, done by Rovithis-Livaniou et al. (2001), we report a larger inclination ($i_{R-L} = 76^\circ$ compared to $82^\circ$ in the present work), a slightly higher temperature of the secondary ($T_{R-L}$=5900 K, compared to 6200 K in this study), and different polar radii of the components, but within our estimated uncertainties.

The distance of the system, according to the absolute magnitude from Table 4, is 103 ± 3 pc. Based on the current mass and luminosity of the secondary component and the methods described by Yıldız (2014), we estimate that the age of AK Her is 4.58 ± 2.51 Gyr.

## 5. HI Dra

HI Dra (HD 171848, BD+58 1824, NSVS 3037033, GSC 03917-02301, ADS 11465 A) is a bright contact binary discovered in the Hipparcos observations and initially classified as an RR Lyr variable. Gomez-Forrellad et al. (1999) published the light curve and suggested that HI Dra may be a $\beta$ Lyr or an ellipsoidal variable, pointing that the difference of 0.02 mag between light curve levels prior and after the primary minimum is indicative of binarity. Selam (2004) re-analyzed the Hipparcos photometric data under the assumption

that the object is a binary system, and determined a photometric mass ratio of 0.15 and an inclination angle of 52.5 degrees.

The first spectroscopic study of HI Dra, done by Pribulla et al. (2009), confirmed the binary nature of the system. The authors calculated the spectroscopic mass ratio of $q = 0.25$, which is the value used in the present work, and determined the spectral class as F0−F2 V.

The results of our analysis of the new $BVR_CI_C$ light curves of HI Dra are summarized in Table 5 and illustrated in Figure 2. Due to the very low inclination ($i = 54^{\circ}$), the light curve is of sinusoidal shape reminiscent of ellipsoidal variables, with minima of nearly equal depth. The slight asymmetry of the light curves is accounted for by adding a bright spot to the primary star in the neck region of the system. Since it is the less massive secondary that is eclipsed in the deeper minimum, this is a W-type W UMa binary with the degree of overcontact of 23%. Within the estimated uncertainty, the primary has a mass that could be expected from a class F0-F2 main sequence star, but a larger radius and luminosity. We find a faint third light in B and $I_C$ bands. Estimated distance of HI Dra, based on the absolute parameters resulting from our analysis, is 304 ± 27 pc, and its age, 2.01 ± 1.18 Gyr.

One of the intermediate results of the age calculation is the initial mass of the secondary component, which in this case 2.14 $M_{\odot}$. According to Yıldız (2014), this indicates that the system should have evolved into an A-subtype W UMa binary. However, when we made trial models with the A-subtype configuration, could not obtain a fit of satisfying quality, and the best solutions in such a case demanded greatly increased temperature of the secondary (in excess of 1000 K above the temperature of the primary), which isn't characteristic of W UMa stars. Therefore, we remain with the more likely classification of HI Dra as a W-subtype system.

## 6. V1128 Tau

V1128 Tau is a W UMa type variable with a visual companion (BD+12 511B) separated by 14 arcsec. Its light curves were studied by Taş et al. (2003), Hawkins et al. (2005) and Zhang (2011) with relatively homogenous conclusions. Using newly measured times of minimum light and all the available data from the literature, Liu et al. (2011) reported a long-term variation of the orbital period, which could be explained by Applegate mechanism on one of the components. Rucinski et al. (2008) performed a radial velocity study and found a mass ratio of $q = 0.534$, which is used in the present work, and estimated a spectral type of F8 V.

Our analysis of the new $BVR_C$ light curves of V1128 Tau is summarized in Table 6 and illustrated in Figure 3. The light curves exhibit continual changes, minima of almost equal depths, and a slight asymmetry between maxima that we account for by putting a dark spot on the secondary component. The mass and radius of the primary are reasonably close to those expected from a main sequence F8 star. Since it is the more massive star that is eclipsed in the deeper minimum, V1128 Tau is a W-type W UMa system. We find that the degree of overcontact is 13.4%, the distance is 139 ± 3 pc, and the age of V1128 Tau is 5.04 ± 1.86 Gyr.

Our results are in good agreement with the most recent photometric study of V1128 Tau done by Zhang (2011), with the exception of the presence of the dark spot; namely, they presented a spotless solution, whereas we were not able to obtain a satisfying fit to the observations without the inclusion of a spot.

### 6.1. O-C analysis

We performed an O-C analysis of V1128 Tau based on the photoelectric and CCD times of minimum light that we collected from the literature and observed ourselves. The O-C diagram (see Fig. 5), displays a cyclic character superimposed on a quadratic variation. The quadratic variation can be explained by the mass exchange/mass loss in the system, while cyclic variation may be the result of the presence of a gravitationally bound third body or magnetic activity on one of the components (see e.g. Selam & Albayrak 2007).

The orbital period decrease of $dP/dt = -3.46 \times 10^{-8}$ day yr$^{-1}$ is indicative of mass transfer from the primary to the secondary component at a rate of $\sim -1.13 \times 10^{-7} M_{\odot} y^{-1}$, unless mass is being lost from the system through some other mechanism, e.g. stellar winds.

Considering a hypothetical third body gravitationally bound to the close binary, we determined the parameters of the light-time orbit as $T_0$, $P_{orb}$, $\frac{dP}{dE}$, $P_{12}$, $T'$, $a'_{12} \sin i'$, $e'$, $\omega'$, using the OC2LTE30 code (Ak et al. 2004), which is based on the formulation by Irwin (1952).

The magnetic activity parameters of the secondary component can be calculated using the formalism of Applegate (1992) as an alternative explanation for the observed cyclic period variation. In this context, the period and amplitude of the cyclic period variation are found to be 12.54 years and 0.105 s cyc$^{-1}$ respectively, while the angular momentum transfer and the energy required for the angular momentum transfer are computed to be $-8.34 \times 10^4 6$ g cm$^2$ s$^{-1}$ and $6.46 \times 10^{40}$ erg. The resulting variations in the luminosity and brightness of the secondary are then $5.13 \times 10^{32}$ erg s$^{-1}$ and $0.^m01$ respectively. All the parameters of the suggested quadratic and cyclic period variations are summarized in Table 8.

The O-C diagram for V1128 Tau, based on all observations made so far, covers one

incomplete cycle of the predicted variation. We thus refrain from drawing any definite coclusions about the mechanism for the suggested cyclic variation. Further observations are needed to understand its nature and origin.

## 7. V2612 Oph

V2612 Oph (HD 170451, BD+06 3809, NSV 10892, GSC 445-1993, NGC 6633-147) is bright ($V_{max} = 6^m.20$) eclipsing binary that was thought to be a member of the galactic cluster NGC 6633 (Hiltner et al. 1958). Its light curves were studied by several groups (Koppelman et al. 2002; Hidas et al. 2005; Yang et al. 2005; Deb et al. 2011). Pribulla et al. (2007) did a spectroscopic analysis and determined the spectral class of the system as F7 V and its mass ratio as $q = 0.286$, which is the value used in the present work. They dispute the cluster membership of V2612 Oph on the basis of the detection of a much fainter ($V = 12^m.8$) W-UMa type cluster member, whereas the brightness of V2612 Oph, when calculated using the distance modulus of NGC 6633 given by Kharchenko et al. (2005), would have to be $V_{max} = 11^m.26$ if it was a member of the cluster.

The new $BVR_CI_C$ light curves of V2612 Oph, along with the best fitting model, are shown in Figure 4, and the summary of our analysis is given in Table 7. There's a significant difference in the height of adjacent maxima, as well as a noticable asymmetry. These features are modeled by placing a dark spot in the polar region of each component. According to Schuessler & Solanki (1992), the presence of spots at high latitudes can be explained by the dynamo mechanism for rapid rotators, and short-period, close binaries can be considered as such. The absolute parameters of the primary are in accordance with its spectral classification as a main sequence star. As the deeper minimum corresponds to the eclipse of the more massive primary star, this is an A-subtype W UMa binary. The degree of overcontact is 22%, the distance is 173 ± 5 pc, and the age of V2612 Oph is 5.11 ± 1.79

Gyr. The distance and age of V2612 Oph indicate that it should not be a member of NGC 6633 cluster, which has a distance of 376 pc and age of 425 Myr (according to WEBDA[3]).

These findings are in good agreement with the results of previous studies, with one exception: Deb et al. (2011) classifies V2612 Oph as a W-subtype W UMa system. Such classification is not supported by our model, which cannot fit the observations well if a W-subtype configuration is attempted.

## 8. Resume

We performed the numerical analysis of four W UMa type overcontact binaries: AK Her, HI Dra, V1128 Tau, and V2612 Oph and determined their absolute physical and orbital parameters. Our results are based on new photometric observations and recent radial velocity studies. The analysis was done using a sophisticated model of a binary system that provided excellent fits to the observations. In addition to updating the ephemeris and the absolute parameters, we calculated the distance and estimated the age of each object, and did an O-C analysis for V1128 Tau that revealed a complex period variation consistent with mass transfer within the system and either the presence of the third body or magnetic activity on one of the components. Unfortunately, at the time of this writing, the available times of minimum light for HI Dra and V2612 Oph do not allow for the construction of an O-C diagram. This could be achieved in the future with further observations, which would help to better understand the nature and variability of these systems, and widen the knowledge about overcontact binary stars in general.

This research was funded in part by the Ministry of Education, Science and Technolog-

[3]http://www.univie.ac.at/webda/

ical Development of Republic of Serbia through the project "Stellar Physics" (No. 176004). The authors acknowledge the use of the [http://simbad.u-strasbg.fr/simbad/]Simbad database, operated at the CDS, Strasbourg, France, [http://adsabs.harvard.edu/]NASA's Astrophysics Data System Bibliographic Services and [http://www.univie.ac.at/webda/] WEBDA database of stellar clusters in the Galaxy and the Magellanic Clouds.

*Facilities:* AUKR.

## REFERENCES

Ak, T., Albayrak, B., Selam, S.O., Tanriverdi, T., 2004, NewA, 9, 265

Applegate, J.H., 1992, ApJ 358, 621

Binnendijk, L., 1970, Vistas in Astronomy, 12, 217

Claret, A., & Bloemen, S., 2011, A&A, 529, 75

Cruddace, R. G. & Dupree, A. K., 1984, ApJ, 277, 263

Deb, S., Singh, H. P., 2011, MNRAS, 412, 178

Djurašević G., 1992, Ap&SS 196, 241

Djurašević G., 1992, Ap&SS 197, 17

Djurašević G., Zakirov M., Hojaev A., Arzumanyants G., 1998, A&A 415, 283

Flower P.J., 1996, AJ, 469, 355

Gomez-Forrellad, J. M., Garcia-Melendo, E., Guarro-Flo, J., Nomen-Torres, J., & Vidal-Sainz, J., 1999, IBVS, 4702, 1

Hawkins, N. C., Samec, R. G., van Hamme, W., & Faulkner, D. R., 2005, IBVS, 5612, 1

Hidas, M. G., Ashley, M. C. B., Webb, J. K., Irwin, M., Phillips, A., Toyozumi, H., Derekas, A., Christiansen, J. L., Nutto, C., & Crothers, S., 2005, MNRAS, 360, 703

Hiltner, W. A., Iriarte, B., & Johnson, H. L., 1958, ApJ, 127, 539

Høg, E., Fabricius, C., Makarov, V. V., Urban, S., Corbin, T., Wycoff, G., Bastian, U. Schwekendiek, P., Wicenec, A., 2000, A&A, 355, 27

Irwin, J.B., 1952, ApJ, 116, 211

Kharchenko, N. V., Piskunov, A. E., Roser, S., Schilbach, E., & Scholz, R.-D., 2005, A&A, 438, 1163

Koppelman, M. D., West, D., & Price, A., 2002, IBVS, 5327, 1

Kwee, K.K., van Woerden, H., 1956 BAN 12, 327

Li, L., Zhang, F. & Han, Z., 2001, A&A, 368, 595

Liu, L., Qian, S.-B., Liao, W.-P., He, J.-J., Zhu, L.-Y., Li, L.-J., & Zhao, E.-G., 2011, Ap&SS, 334, 131

Lucy L. B., 1967, Zeitschritft fur Astrophysik, 65, 89

Marquardt D. W., 1963, J. Soc. Ind. Appl. Math. 11 (2), 431

Martins F., Schaerer D., Hillier D. J., 2005, A&A, 436, 1049

McGale, P. A., Pye, J. P. & Hodgkin, S. T., 1996, MNRAS, 280, 627

Pribulla, T., Rucinski, S., Lu, W., Mochnacki, S., Conidis, G., Blake, R., DeBond, H., Thomson, J., Pych, W., Ogloza, W., Siwak, M., 2006, AJ, 132, 769

Pribulla, T., Rucinski, Conidis, G., DeBond, H., Thomson, J., Kosmas, G., Ogloza, W., 2007, AJ, 133, 1977

Pribulla, T., Rucinski, S., Blake, R., Lu, W., Thomson, J., DeBond, H., Karmo, T., De Ridder, A., Ogloza, W., Stachowski, G., Siwak, M., 2009, AJ, 137, 3655

Rovithis-Livaniou, H., Fragoulopoulou, E., Sergis, N., Rovithis, P., & Kranidiotis, A., 2001, Ap&SS, 275, 337

Rucinski, S., Pribulla, T., Mochnacki, S., Liokumovich, E., Lu, W., DeBond, H., De Ridder, A., Karmo, T., Rock, M., Thomson, J., Ogloza, W., Kaminski, K., Ligeza, P., 2008, AJ, 136, 586

Samadi, A., Jassur, D. M. Z., Nassiri, S., Gozaliasl, G., Kermani, M. H. & Zareie, A., 2010, NewA, 15, 339

Samus, N. N., Goranskii, V. P., Durlevich, O. V., Zharova, A. V., Kazarovets, E. V., Kireeva, N. N., Pastukhova, E. N., Williams, D. B., Hazen, M. L., 2003, Astronomy Letters, 29, 468

Sanford, R. F., 1934, ApJ, 79, 89

Schlegel D. J., Finkbeiner D. P., Davis M., 1998, AJ, 500, 525

Schmidt, H. & Herczeg, T., 1959, ZA, 47, 106

Schuessler, M. & Solanki, S. K., 1992, A&A, 264L, 13

Selam, S. O., 2004, A&A, 416, 1097

Selam, S. O., & Albayrak, B., 2007, AN, 328, 2, 154

Taş, G., Evren, S., Çakirli, Ö, & Íbanoğlu, C., 2003, A&A, 411, 161

van Leeuwen, F., 2007, A&A, 474, 653

von Zeipel H., 1924, MNRAS, 84, 665

Woodward, E., 1941, PhD Thesis, Radcliffe College

Yang, Y.-G., Qian, S.-B., & Koppelman, M. D., 2005, ChJAA, 5, 137

Yıldız, M., 2013, MNRAS, 437, 185

Zhang, X.-B., Ren, A.-B., Luo, C.-Q., & Luo, Y.-P., 2011, RAA, 11, 583

This manuscript was prepared with the AAS LaTeX macros v5.2.

Table 1: Summary of observational aspects.

| Program star | Comparison star | Light curve $\sigma$ | | | | Epoch [HJD] | Period [days] |
|---|---|---|---|---|---|---|---|
| | | B | V | R | I | | |
| AK Her | PPM 133147 | 0.152 | 0.144 | 0.144 | 0.133 | 2453176.393(9) | 0.421523(2) |
| HI Dra | GSC 3917-1556 | 0.057 | 0.058 | 0.058 | 0.056 | 2456534.419(2) | 0.597423(2) |
| V1128 Tau | GSC 664-387 | 0.243 | 0.226 | 0.221 | — | 2454842.3470(1) | 0.305371(2) |
| V2612 Oph | GSC 445-1293 | 0.126 | 0.119 | 0.115 | 0.112 | 2453846.916(1) | 0.375307(3) |

Table 2: New times of minimum light derived from our observations.

| System | Time of minimum [HJD] | Type |
|---|---|---|
| AK Her | 2456512.3234(3) | Primary |
| | 2456516.3284(1) | Secondary |
| HI Dra | 2456526.3530(1) | Secondary |
| | 2456534.4190(2) | Primary |
| | 2456372.5190(1) | Primary |
| V1128 Tau | 2454785.3952(1) | Secondary |
| | 2454813.4894(1) | Secondary |
| | 2454842.1949(1) | Secondary |
| | 2454842.3480(1) | Primary |
| V2612 Oph | 2456517.4112(1) | Secondary |
| | 2456519.2882(1) | Secondary |
| | 2456530.3591(2) | Primary |

Table 3: BVRI Photometry of AK Her, HI Dra, V1128 Tau, V2612 Oph

| AK Her: $B$ band | | |
|---|---|---|
| HJD (d) | Phase | Diff. Magnitude (mag) |
| 2456510.2891 | 0.1714 | -1.006 |
| 2456510.2905 | 0.1747 | -1.013 |
| 2456510.2919 | 0.1781 | -1.017 |
| 2456510.2933 | 0.1814 | -1.016 |
| 2456510.2947 | 0.1848 | -1.019 |

Note. — This table is available in its entirety in machine-readable and Virtual Observatory (VO) forms in the online journal. A portion is shown here for guidance regarding its form and content.

Table 4: Summary of modeling results for AK Her.

| Properties of the fit | | |
|---|---|---|
| Point count | 1407 | |
| $\sigma$ | 0.0097 | |
| **System parameters** | | |
| q | 0.277 ± 0.024 | |
| i [°] | 81.7 ± 0.2 | |
| $a_{orb}$ [$R_\odot$] | 2.73 ± 0.09 | |
| d [pc] | 103 ± 3 | |
| $f_{over}$[%] | 33.2 | |
| $\Omega_{in}, \Omega_{out}$ | 2.4148, 2.2412 | |
| $\ell_3/(\ell_1+\ell_2+\ell_3)$ | 0.102 ± 0.002 [B], 0.130 ± 0.002 [V], 0.146 ± 0.002 [$R_C$], 0.162 ± 0.003 [$I_C$] | |
| **Stellar Parameters** | **Primary** | **Secondary** |
| A | 0.5 | 0.5 |
| $\beta$ | 0.08 | 0.08 |
| f | 1.0 | 1.0 |
| $T_{eff}$ [K] | 6500 | 6180 ± 10 |
| F | 1.027 ± 0.001 | 1.027 ± 0.001 |
| $\Omega$ | 2.3572 | 2.3572 |
| $L/(L_1+L_2)$ | 0.786 [B], 0.782 [V], 0.780 [$R_C$], 0.778 [$I_C$] | 0.214 [B], 0.218 [V], 0.220 [$R_C$], 0.222 [$I_C$] |
| R [D=1] | 0.475 | 0.269 |
| L [$L_\odot$] | 3.02 ± 0.02 | 0.82 ± 0.02 |
| $\mathcal{M}$ [$M_\odot$] | 1.2 ± 0.2 | 0.34 ± 0.07 |
| $\mathcal{R}$ [$R_\odot$] | 1.40 ± 0.05 | 0.80 ± 0.03 |
| $\log_{10}$(g) | 4.23 ± 0.08 | 4.2 ± 0.2 |
| $M_{bol}$ | 3.54 ± 0.07 | 4.96 ± 0.08 |
| **Spot parameters** | **Spot 1 (Primary)** | **Spot 2 (Primary)** |
| $T_{spot}/T$ | 0.807 ± 0.004 | 0.810 ± 0.06 |
| $\theta$ [°] | 22.1 ± 0.2 | 16.1 ± 0.2 |
| $\lambda$ [°] | 54.6 ± 0.7 | 319 ± 2 |
| $\varphi$ [°] | -37.9 ± 0.6 | -1 ± 2 |

Table 5: Summary of modeling results for HI Dra.

| Properties of the fit | | |
|---|---|---|
| Point count | 2491 | |
| $\sigma$ | 0.0076 | |
| **System parameters** | | |
| q | $0.250 \pm 0.005$ | |
| i [°] | $54.74 \pm 0.05$ | |
| $a_{orb}$ [$R_\odot$] | $3.8 \pm 0.2$ | |
| d [pc] | $304 \pm 27$ | |
| $f_{over}$[%] | 23.0 | |
| $\Omega_{in}, \Omega_{out}$ | 2.3529, 2.1952 | |
| $\ell_3/(\ell_1+\ell_2+\ell_3)$ | $0.032 \pm 0.004$ [B], $0.000 \pm 0.004$ [V], $0.000 \pm 0.004$ [$R_C$], $0.044 \pm 0.004$ [$I_C$] | |
| **Stellar Parameters** | **Primary** | **Secondary** |
| A | 0.5 | 0.5 |
| $\beta$ | 0.08 | 0.08 |
| f | 1.0 | 1.0 |
| $T_{eff}$ [K] | 7000 | $6550 \pm 20$ |
| F | $1.017 \pm 0.001$ | $1.017 \pm 0.001$ |
| $\Omega$ | 2.3167 | 2.3167 |
| $L/(L_1+L_2)$ | 0.822 [B], 0.818 [V], 0.815 [$R_C$], 0.813 [$I_C$] | 0.178 [B], 0.182 [V], 0.185 [$R_C$], 0.187 [$I_C$] |
| R [D=1] | 0.478 | 0.257 |
| L [$L_\odot$] | $7.87 \pm 0.04$ | $1.80 \pm 0.05$ |
| $\mathcal{M}$ [$M_\odot$] | $1.7 \pm 0.3$ | $0.42 \pm 0.07$ |
| $\mathcal{R}$ [$R_\odot$] | $1.97 \pm 0.09$ | $1.07 \pm 0.05$ |
| $\log_{10}$(g) | $4.1 \pm 0.1$ | $4.0 \pm 0.2$ |
| $M_{bol}$ | $2.5 \pm 0.1$ | $4.1 \pm 0.2$ |
| **Spot parameters** | **Spot 1 (Primary)** | |
| $T_{spot}/T$ | $1.139 \pm 0.002$ | |
| $\theta$ [°] | $15.5 \pm 0.2$ | |
| $\lambda$ [°] | $5.0 \pm 0.3$ | |
| $\varphi$ [°] | $6.8 \pm 0.4$ | |

Table 6: Summary of modeling results for V1128 Tau.

| Properties of the fit | | |
|---|---|---|
| Point count | 1865 | |
| $\sigma$ | 0.0098 | |
| **System parameters** | | |
| q | $0.534 \pm 0.006$ | |
| i [°] | $86.0 \pm 0.2$ | |
| $a_{orb}$ [$R_\odot$] | $2.27 \pm 0.04$ | |
| d [pc] | $139 \pm 3$ | |
| $f_{over}$[%] | 13.4 | |
| $\Omega_{in}, \Omega_{out}$ | 2.9406, 2.6240 | |
| **Stellar Parameters** | **Primary** | **Secondary** |
| A | 0.5 | 0.5 |
| $\beta$ | 0.08 | 0.08 |
| f | 1.0 | 1.0 |
| $T_{eff}$ [K] | 6200 | $6400 \pm 10$ |
| F | $1.017 \pm 0.001$ | $1.017 \pm 0.001$ |
| $\Omega$ | 2.8982 | 2.8982 |
| $L/(L_1 + L_2)$ | 0.603 [B], 0.606 [V], 0.608 [$R_C$] | 0.397 [B], 0.394 [V], 0.392 [$R_C$] |
| R [D=1] | 0.416 | 0.312 |
| L [$L_\odot$] | $1.294 \pm 0.009$ | $0.839 \pm 0.008$ |
| $\mathcal{M}$ [$M_\odot$] | $1.10 \pm 0.06$ | $0.58 \pm 0.04$ |
| $\mathcal{R}$ [$R_\odot$] | $1.01 \pm 0.02$ | $0.76 \pm 0.02$ |
| $\log_{10}$(g) | $4.47 \pm 0.04$ | $4.44 \pm 0.04$ |
| $M_{bol}$ | $4.46 \pm 0.04$ | $4.93 \pm 0.04$ |
| **Spot parameters** | **Spot 1 (Secondary)** | |
| $T_{spot}/T$ | $0.869 \pm 0.006$ | |
| $\theta$ [°] | $24.8 \pm 0.5$ | |
| $\lambda$ [°] | $146 \pm 3$ | |
| $\varphi$ [°] | $52 \pm 2$ | |

Table 7: Summary of modeling results for V2612 Oph.

| Properties of the fit | | |
|---|---|---|
| Point count | 1363 | |
| $\sigma$ | 0.0074 | |
| **System parameters** | | |
| q | $0.286 \pm 0.003$ | |
| i [°] | $66.66 \pm 0.05$ | |
| $a_{orb}$ [$R_\odot$] | $2.59 \pm 0.07$ | |
| d [pc] | $173 \pm 5$ | |
| $f_{over}$ [%] | 22.1 | |
| $\Omega_{in}$, $\Omega_{out}$ | 2.4351, 2.2562 | |
| $\ell_3/(\ell_1+\ell_2+\ell_3)$ | $0.000 \pm 0.002$ [B], $0.004 \pm 0.002$ [V], $0.000 \pm 0.003$ [$R_C$], $0.025 \pm 0.003$ [$I_C$] | |
| **Stellar Parameters** | **Primary** | **Secondary** |
| A | 0.5 | 0.5 |
| $\beta$ | 0.08 | 0.08 |
| f | 1.0 | 1.0 |
| $T_{eff}$ [K] | 6250 | $6280 \pm 10$ |
| F | $1.018 \pm 0.001$ | $1.018 \pm 0.001$ |
| $\Omega$ | 2.3956 | 2.3956 |
| $L/(L_1+L_2)$ | 0.751 [B], 0.751 [V], 0.752 [$R_C$], 0.752 [$I_C$] | 0.249 [B], 0.249 [V], 0.248 [$R_C$], 0.248 [$I_C$] |
| R [D=1] | 0.468 | 0.267 |
| L [$L_\odot$] | $2.23 \pm 0.02$ | $0.75 \pm 0.01$ |
| $\mathcal{M}$ [$M_\odot$] | $1.3 \pm 0.1$ | $0.37 \pm 0.04$ |
| $\mathcal{R}$ [$R_\odot$] | $1.30 \pm 0.04$ | $0.75 \pm 0.01$ |
| $\log_{10}$(g) | $4.32 \pm 0.06$ | $4.25 \pm 0.06$ |
| $M_{bol}$ | $3.87 \pm 0.06$ | $5.05 \pm 0.06$ |
| **Spot parameters** | **Spot 1 (Primary)** | **Spot 2 (Secondary)** |
| $T_{spot}/T$ | $0.798 \pm 0.003$ | $0.807 \pm 0.005$ |
| $\theta$ [°] | $28.3 \pm 0.3$ | $37.9 \pm 0.2$ |
| $\lambda$ [°] | $168.7 \pm 0.6$ | $329.1 \pm 0.5$ |
| $\varphi$ [°] | $77.9 \pm 0.2$ | $33 \pm 1$ |

Table 8: Parameters derived from the O-C analysis of V1128 Tau.

| Parameters | Values |
|---|---|
| $T_0$ [HJD] | $2454842.3470 \pm 0.0001$ |
| $P_{orb}$ [day] | $0.305371 \pm 0.0000001$ |
| $\frac{dP}{dE}$ [day/cyc] | $-3.10 \pm 0.02 \times 10^{-10}$ |
| $a_{12}^{'} \sin i^{'}$ [AU] | $0.53 \pm 0.04$ |
| $e^{'}$ | $0.3 \pm 0.2$ |
| $\omega^{'}$ [°] | $56 \pm 14$ |
| $T^{'}$ [HJD] | $2456290 \pm 50$ |
| $P_{12}$ [year] | $12.6 \pm 0.3$ |
| $A$ [day] | $0.0030 \pm 0.0002$ |
| $f(m_3)$ [$M_\odot$] | $0.0009 \pm 0.0002$ |
| $M_3$ [$M_\odot$] | $0.15 \pm 0.01$ |

Note. —

- $A$ — the semi-amplitude of the light-time effect.
- $T^{'}$ — the periastron passage.
- $P_{12}$ — the period of the hypothetical third body.
- $a_{12}^{'} \sin i^{'}$ — the semi-major axis.
- $e^{'}$ — the eccentricity.
- $\omega^{'}$ — the longitude of the periastron passage of the orbit of the eclipsing pair around the mass center of the system.
- $f(m_3)$ — the mass function for the hypothetical third body.
- $M_3$ — the mass of the hypothetical third body.

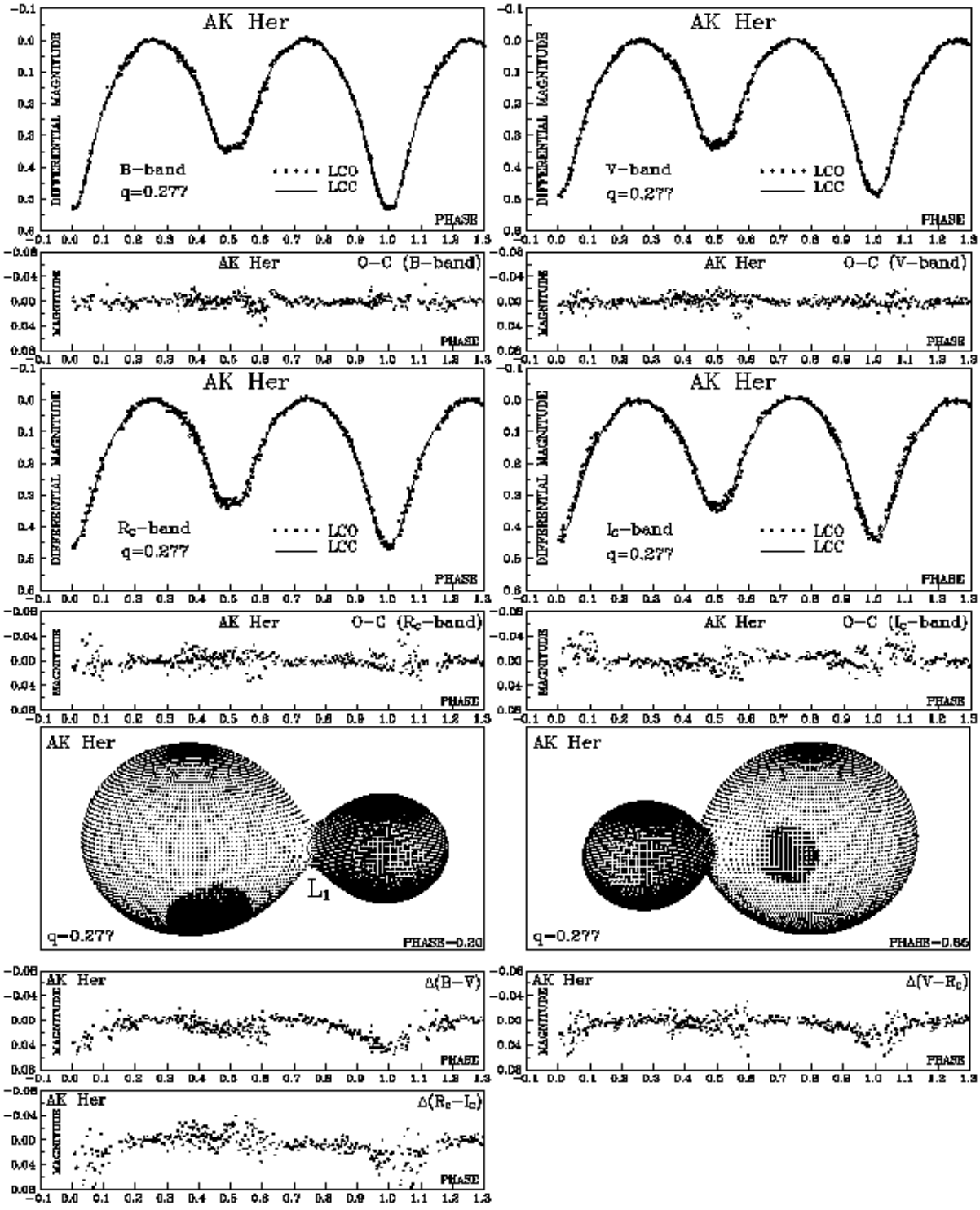


Fig. 1.— Observed (LCO) and synthetic (LCC) light curves and the final O-C residuals of AK Her, with $\Delta(B-V)$, $\Delta(V-R_C)$ and $\Delta(R_C-I_C)$ color curves and the graphic representation of the model described in Section 4 at the orbital phases 0.20 and 0.85.

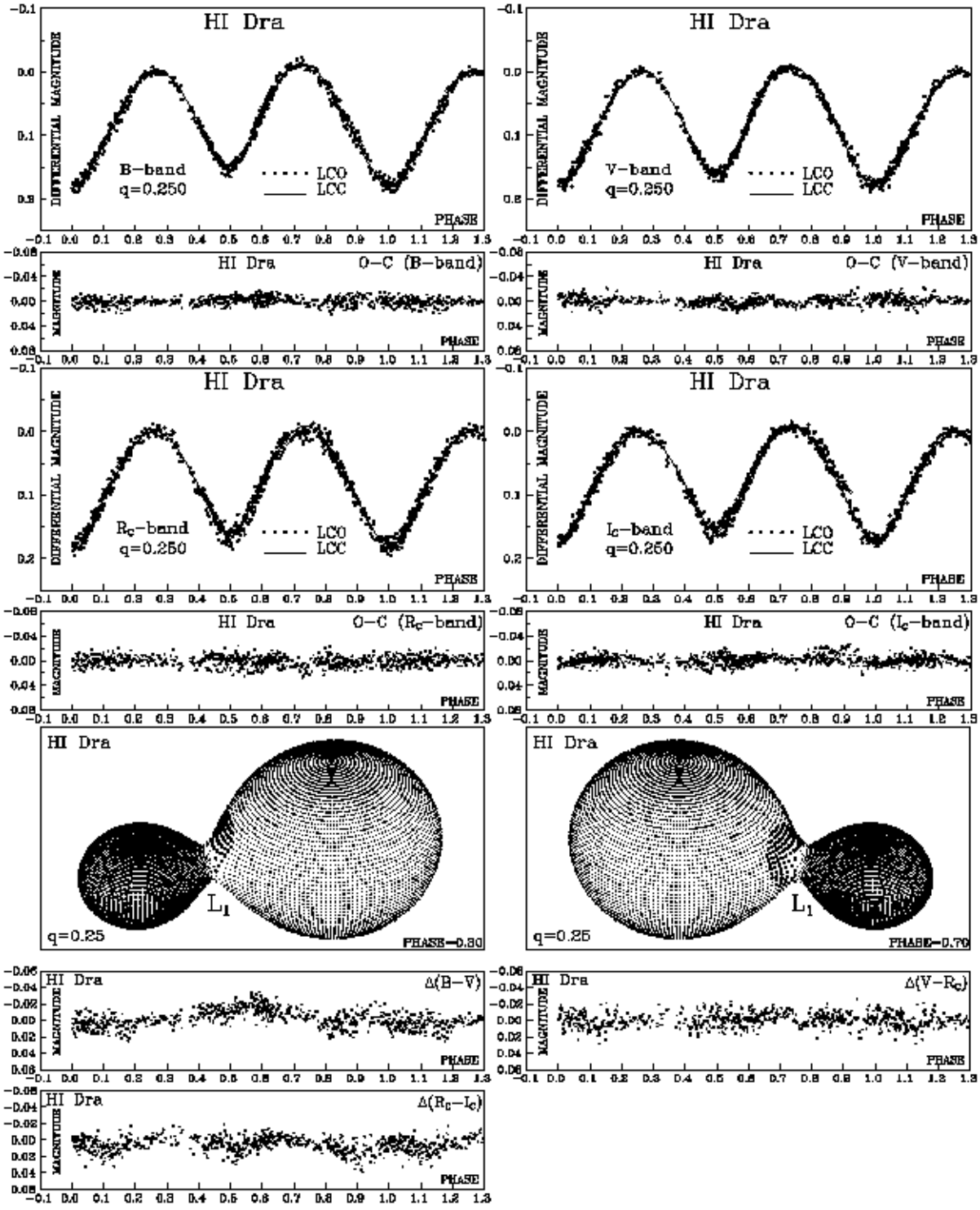


Fig. 2.— Observed (LCO) and synthetic (LCC) light curves and the final O-C residuals of HI Dra, with $\Delta(B-V)$, $\Delta(V-R_C)$ and $\Delta(R_C-I_C)$ color curves and the graphic representation of the model described in Section 5 at orbital phases 0.30 and 0.70.

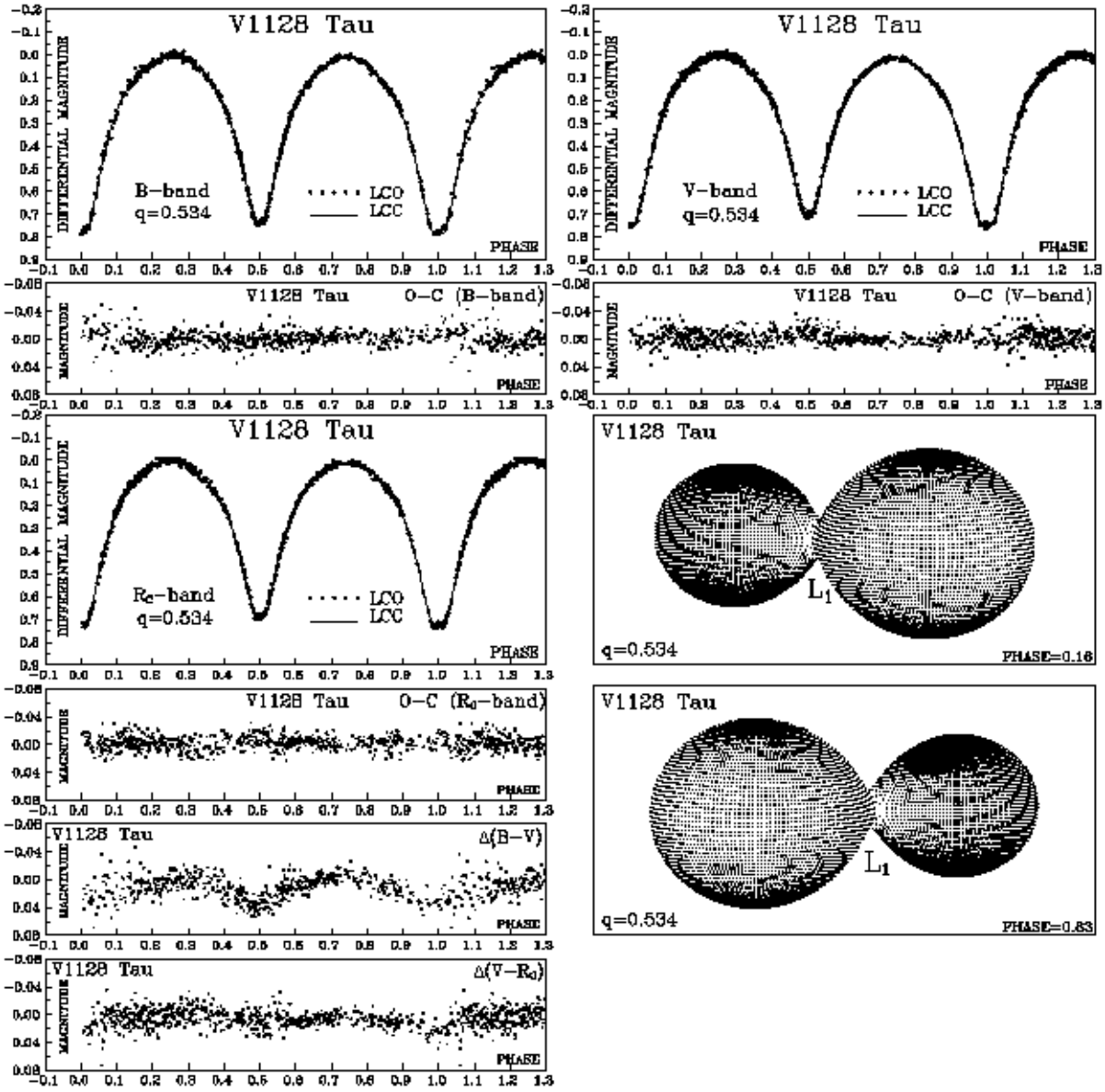


Fig. 3.— Observed (LCO) and synthetic (LCC) light curves and the final O-C residuals of V1128 Tau, with $\Delta(B-V)$ and $\Delta(V-R_C)$ color curves and the graphic representation of the model described in Section 6 at orbital phases 0.16 and 0.83.

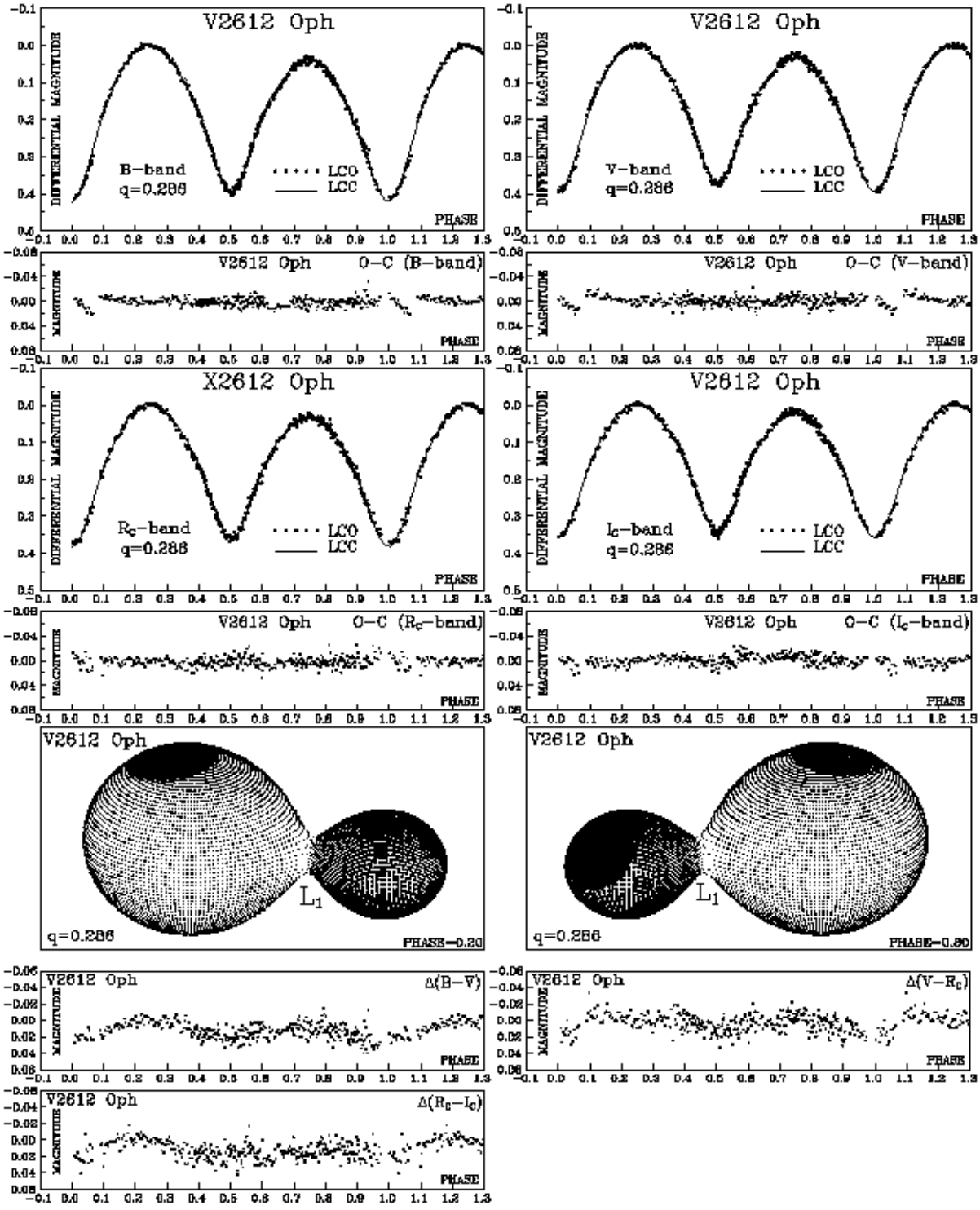


Fig. 4.— Observed (LCO) and synthetic (LCC) light curves and the final O-C residuals of V2612 Oph, with $\Delta(B-V)$, $\Delta(V-R_C)$ and $\Delta(R_C-I_C)$ color curves and the graphic representation of the model described in Section 7 at orbital phases 0.20 and 0.80.

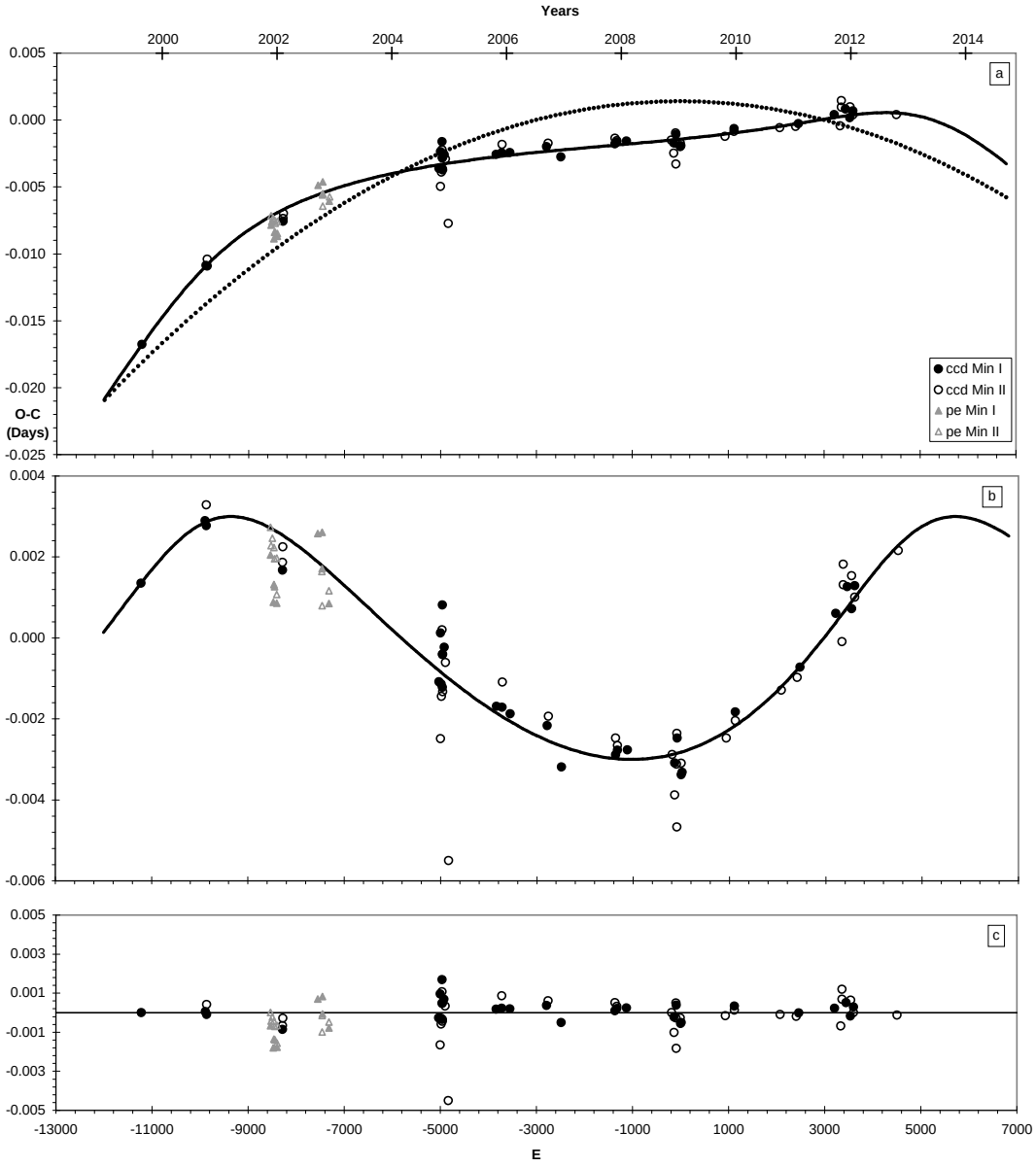


Fig. 5.— (a) The O-C diagram for V1128 Tau with the photoelectric (gray triangles) and CCD (black circles) times of minima. The dotted and solid curves show the quadratic and overall (quadratic plus cyclic) parts of the fitted function. (b) The residuals from the quadratic fit; the solid curve represents the cyclic part of the fitted function. (c) The O-C residuals after the subtraction of the fitted function.